nature medicine

CD47 blockade triggers T cell–mediated destruction of immunogenic tumors

Xiaojuan Liu[1,2,6], Yang Pu[3], Kyle Cron[3], Liufu Deng[3], Justin Kline[4], William A Frazier[5], Hairong Xu[1], Hua Peng[1], Yang-Xin Fu[1,3,7] & Meng Michelle Xu[3,6,7]

Macrophage phagocytosis of tumor cells mediated by CD47-specific blocking antibodies has been proposed to be the major effector mechanism in xenograft models. Here, using syngeneic immunocompetent mouse tumor models, we reveal that the therapeutic effects of CD47 blockade depend on dendritic cell but not macrophage cross-priming of T cell responses. The therapeutic effects of anti-CD47 antibody therapy were abrogated in T cell–deficient mice. In addition, the antitumor effects of CD47 blockade required expression of the cytosolic DNA sensor STING, but neither MyD88 nor TRIF, in CD11c$^+$ cells, suggesting that cytosolic sensing of DNA from tumor cells is enhanced by anti-CD47 treatment, further bridging the innate and adaptive responses. Notably, the timing of administration of standard chemotherapy markedly impacted the induction of antitumor T cell responses by CD47 blockade. Together, our findings indicate that CD47 blockade drives T cell–mediated elimination of immunogenic tumors.

Phagocytosis relies on a balance between prophagocytic ("eat me") and antiphagocytic ("don't eat me") signals on target cells[1–3]. CD47, initially observed on stem cells, is a transmembrane protein that inhibits phagocytosis by binding to its receptor, signal regulatory protein α (SIRPα), which is expressed on phagocytes[4–6]. Lack of CD47 on erythrocytes, platelets and lymphohematopoetic cells results in rapid clearance of these cells by macrophages, due to elimination of the CD47-SIRPα–mediated antiphagocytic signal[4,5,7,8]. Binding of CD47 to SIRPα results in phosphorylation of immunoreceptor tyrosine-based inhibitory motifs (ITIMs) on SIRPα and recruitment of Src homology phosphatases 1 and 2 (SHP-1 and SHP-2), both of which inhibit accumulation of myosin-IIA at the phagocytic synapse[9].

Abundant CD47 expression has also been observed on a variety of malignant cells, including both hematopoietic and solid tumors, especially tumor-initiating cells, where elevated CD47 expression has predicted poor survival in individuals with cancer[10–14]. These data provide a strong rationale for therapeutic targeting of CD47 (refs. 12,15). Human CD47-blocking monoclonal antibodies (mAbs) have demonstrated efficacy in various preclinical models of human lymphoma, bladder cancer, colon cancer, glioblastoma, breast cancer, acute lymphocytic leukemia and acute myeloid leukemia[11,12,16–18]. Most work concluded that the therapeutic effects of anti-human CD47 were macrophage dependent. However, these studies employed xenografted human tumors in T cell–deficient mice[16,18,19]. Thus, they were not able to evaluate the role of adaptive immunity in the effectiveness of CD47 blockade. A previous study showed that morpholino-mediated knockdown of CD47 on tumors in wild-type (WT) mice enhanced the tumoricidal activity of CD8$^+$ T cells when combined with irradiation[20]. But irradiation alone is known to stimulate antitumor CD8$^+$ T cell responses[21]. Therefore, it remains unclear how CD47 knockdown or antibody-mediated blockade alone controls tumor growth in an immunocompetent host harboring a syngeneic tumor.

Here we show that the therapeutic effect of CD47 blockade in syngeneic tumor models largely depends on the activation of T cells. More specifically, we demonstrate that the therapeutic effects of anti-CD47 relies on a cytosolic DNA sensor, dendritic cells (DCs), type I/II interferons (IFNs) and CD8$^+$ T cells. As such, we conclude that anti-CD47–mediated tumor rejection requires both innate and adaptive immune responses.

RESULTS

T cells are essential for anti-CD47–mediated tumor regression

To evaluate whether treatment with an anti-mouse-CD47 mAb (anti-CD47: MIAP301), known to functionally inhibit CD47-SIRPα interactions, could reduce tumor burden in syngeneic WT mice, we subcutaneously (s.c.) inoculated BALB/c mice with CD47$^+$ A20 B cell lymphoma cells. Seven days later, we administered anti-CD47 intraperitoneally (i.p.) and monitored tumor growth. Compared to isotype control antibody treatment, systemic anti-CD47 treatment slowed the growth of tumor and prolonged the survival of mice bearing immunogenic A20 tumors (**Fig. 1a** and **Supplementary Fig. 1a**). To extend these findings to a solid tumor model, we treated syngeneic C57BL/6 mice bearing established MC38 tumors in a similar manner and observed similar results (**Supplementary Fig. 1b**,**c**). To focus

[1]Institute of Biophysics and the University of Chicago Joint Group for Immunotherapy, Chinese Academy of Science Key Laboratory for Infection and Immunity, Institute of Biophysics, Chinese Academy of Sciences, Beijing, China. [2]University of Chinese Academy of Sciences, Beijing, China. [3]Department of Pathology and Committee on Immunology, University of Chicago, Chicago, Illinois, USA. [4]Department of Medicine and Committee on Immunology, University of Chicago, Chicago, Illinois, USA. [5]Department of Biochemistry and Molecular Biophysics, Washington University, St. Louis, Missouri, USA. [6]These authors contributed equally to this work. [7]These authors jointly supervised this work. Correspondence should be addressed to Y.-X.F. (yfu@uchicago.edu).

Received 8 June; accepted 23 July; published online 31 August 2015; doi:10.1038/nm.3931

on the effect of anti-CD47 within the tumor microenvironment and rule out any effect on peripheral tissues, we administered anti-CD47 by intratumoral injection in both the A20 and MC38 models (**Fig. 1b**,**c**). After only two low doses of anti-CD47, established tumors completely regressed. Because anti-CD47 might have off-target effects[22], we employed a high-affinity Sirpα variant human Fc fusion protein (SIRPα-hIg) as a second approach to antagonize CD47-SIRPα interactions *in vivo*[23]. Consistently, intratumoral blockade of CD47-SIPRα interactions via this approach recapitulated the inhibition of A20 tumor growth triggered by antibody-mediated CD47 blockade (**Fig. 1d**).

We next addressed the extent to which the antitumor effect of CD47 blockade depended on host T cells. Thus, we inoculated A20 lymphoma cells s.c. into syngenic BALB/c nude mice. The same short course of intratumoral anti-CD47 treatment that was efficacious in WT BALB/c mice had no effect on tumor growth in T cell–deficient nude mice (**Fig. 1e**). Although a longer course of consecutive intratumoral anti-CD47 administrations resulted in a transient suppression of tumor growth in tumor-bearing nude mice (**Fig. 1f**), T cells were clearly required for a maximal therapeutic effect of CD47 blockade therapy.

To understand which T cell subsets were involved in anti-CD47–mediated tumor reduction, we treated WT mice bearing established A20 tumors with anti-CD47 intratumorally in conjunction with $CD8^+$ or $CD4^+$ T cell depletion achieved by intraperitoneal delivery of anti-CD4 or anti-CD8 mAbs. In the absence of $CD8^+$ T cells, the therapeutic effect of anti-CD47 was completely abrogated, whereas depletion of $CD4^+$ T cells had no effect (**Fig. 2a**). $CD8^+$ or $CD4^+$ T cells were also depleted in mice systemically treated with anti-CD47. These tumors grew faster in the absence of $CD8^+$ T cells, indicating that this T cell subset is required for tumor regression also following systemic CD47 blockade (**Supplementary Fig. 2a**,**b**).

To determine whether the immune response initiated by anti-CD47 treatment resulted in T cell–mediated memory response against tumor antigens, we rechallenged mice that had rejected A20 lymphomas after an initial course of CD47 blockade (tumor-free >30 days) with a higher dose of A20 cells (2.5×10^7 cells) in the contralateral flank. Compared to naive mice, in which a primary A20 cell challenge resulted in rapid tumor progression, those that had rejected an initial tumor challenge after CD47 blockade were completely resistant to a rechallenge with A20 cells (**Fig. 2b**). These results clearly demonstrate that anti-CD47 treatment can elicit durable systemic immune memory to prevent relapse.

To determine whether anti-CD47 treatment can enhance tumor antigen–specific T cell responses, we treated mice harboring established ovalbumin (OVA)-expressing MC38 tumors with anti-CD47 or isotype control antibody intratumorally. Five days after CD47 blockade, we re-stimulated cells from the tumor-draining lymph node *in vitro* with or without the OVA-derived SIINFEKL peptide and measured IFN-γ production by enzyme-linked immunospot (ELISPOT) assay. Significantly more IFN-γ spot-forming cells were present in the anti-CD47–treated versus the isotype control antibody–treated group (**Fig. 2c**). We observed similar results in the A20 model, where we used irradiated A20 cells to re-stimulate tumor-draining lymph node cells *in vitro* (**Fig. 2d**). To determine whether IFN-γ was essential for the therapeutic effect of anti-CD47, we treated mice bearing A20 tumors with IFN-γ–blocking antibodies on the day of anti-CD47 treatment. The therapeutic effect of anti-CD47 was completely lost in IFN-γ–deficient mice (**Fig. 2e**). Collectively, these data suggest that an antigen-specific T cell response is enhanced after anti-CD47 treatment for both carcinoma and lymphoma tumor types.

Anti-CD47 enhances DC cross-priming for tumor control

A recent study demonstrated that macrophages, and not DCs, were the major antigen-presenting cells (APCs) that cross-prime $CD8^+$ T cells after CD47 blockade in an *in vitro* xenoculture system[24]. To verify these results, we used an *in vitro* syngeneic culture system in which both bone marrow–derived macrophages (BMDMs) and bone marrow–derived DCs (BMDCs) were probed for their ability to cross-prime $CD8^+$ T cells in the presence or absence of anti-CD47.

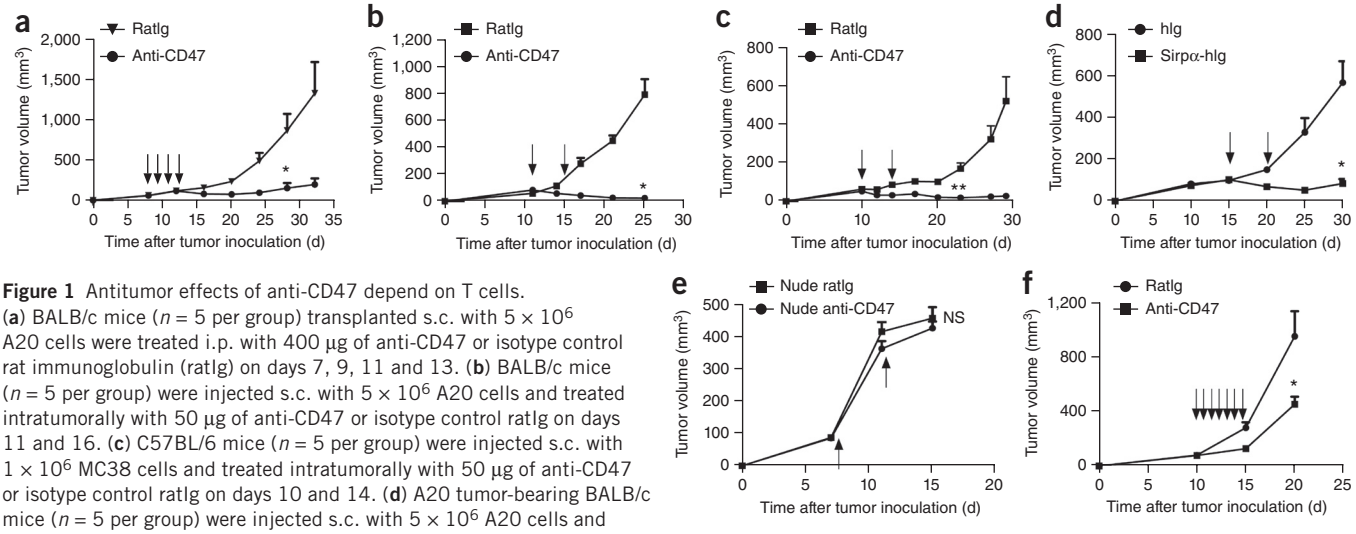

Figure 1 Antitumor effects of anti-CD47 depend on T cells. (**a**) BALB/c mice ($n = 5$ per group) transplanted s.c. with 5×10^6 A20 cells were treated i.p. with 400 μg of anti-CD47 or isotype control rat immunoglobulin (ratIg) on days 7, 9, 11 and 13. (**b**) BALB/c mice ($n = 5$ per group) were injected s.c. with 5×10^6 A20 cells and treated intratumorally with 50 μg of anti-CD47 or isotype control ratIg on days 11 and 16. (**c**) C57BL/6 mice ($n = 5$ per group) were injected s.c. with 1×10^6 MC38 cells and treated intratumorally with 50 μg of anti-CD47 or isotype control ratIg on days 10 and 14. (**d**) A20 tumor-bearing BALB/c mice ($n = 5$ per group) were injected s.c. with 5×10^6 A20 cells and treated twice with 50 μg of high-affinity Sirpα variant Fc fusion protein (Sirpα-hIg) or human Ig intratumorally on days 15 and 20. (**e**) BALB/c nude mice ($n = 4$ per group) were injected s.c. with 2×10^6 A20 cells and intratumorally injected with 50 μg of anti-CD47 or isotype control ratIg on days 7 and 11. (**f**) 2×10^6 A20 cells were transplanted s.c. onto BALB/c nude mice. When tumors were established (>50 mm^3), treatment began with daily intratumoral injections of 50 μg anti-CD47 or 50 μg ratIg for 1 week starting at day 10. Tumor growth is monitored twice a week and reported as the mean tumor size ± s.e.m. over time. One representative experiment out of three (**b**,**c**) or two (**a**,**d**–**f**) yielding similar results is depicted. NS, not significant. $^*P < 0.05$, $^{**}P < 0.01$ (unpaired Student's *t*-test) compared to tumors treated with ratIg. For all panels, the arrow indicates treatment time for anti-CD47.

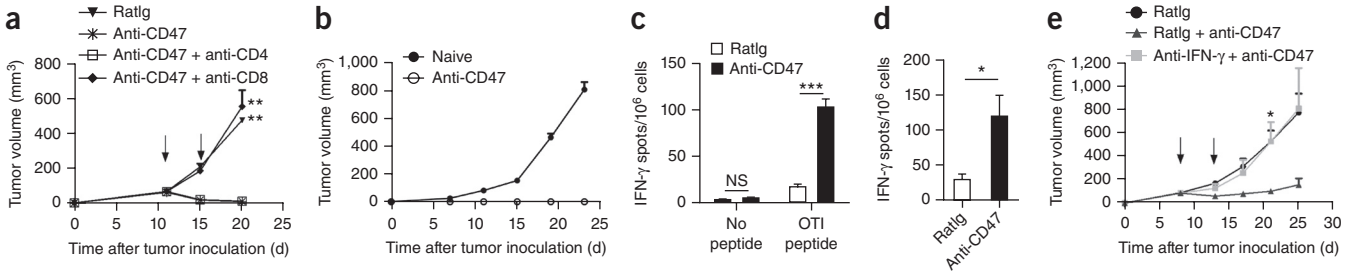

Figure 2 Therapeutic effect of anti-CD47 requires CD8$^+$ T cells. (**a**) BALB/c ($n = 8$ per group) mice were injected s.c. with 5×10^6 A20 cells and treated intratumorally with 50 μg of anti-CD47 or ratIg on days 11 and 15 (indicated by black arrow). Twice a week, 200 μg of CD8- or CD4-depleting antibody was administered, starting on day 11. (**b**) Tumor-free, antibody-treated BALB/c mice ($n = 7$ per group) were rechallenged s.c. with 2.5×10^7 A20 cells on the opposite site from the primary tumor 1 month after complete rejection. (**c**) MC38-OTIp tumor–bearing ($n = 6$ per group) C57BL/6 mice were intratumorally treated twice with 50 μg of either anti-CD47 or ratIg on days 11 and 14. After 5 days, lymphocytes from the DLN were isolated and stimulated with 10 μg/ml OTI peptide. IFN-γ–producing cells were enumerated by ELISPOT assay. (**d**) BALB/c mice ($n = 3$) were injected s.c. with 5×10^6 A20 cells and intratumorally treated with 50 μg of either anti-CD47 or ratIg antibody on days 11 and 16. Seven days after the final treatment, 2×10^5 DLN cells from mice treated with anti-CD47 or ratIg were stimulated with A20 tumor cells irradiated with 60 Gy. The ratio of DLN cells to irradiated tumor was 5:1. IFN-γ–producing cells were enumerated by ELISPOT assay. (**e**) A20 tumor–bearing mice ($n = 5$ per group) were treated twice with 50 μg of anti-CD47 or ratIg intratumorally on days 8 and 13 (indicated by black arrow). 300 μg anti-IFN-γ or ratIg isotype control were injected i.p. every 4 d. Data are reported as the means ± s.e.m. of tumor growth over time. $^*P < 0.05$, $^{**}P < 0.01$, $^{***}P < 0.001$ (unpaired Student's *t*-test). One of three independent experiments is shown.

Whereas anti-CD47 did not significantly increase the cross-priming abilities of BMDMs, BMDCs were able to cross-prime CD8$^+$ T cells to a greater extent than BMDMs in general, but particularly in the presence of anti-CD47 (**Fig. 3a**).

To evaluate the cross-priming capacity of DC and macrophages in response to anti-CD47 *in vivo*, we collected DCs and macrophages from either the MC38 tumor microenvironment or draining lymph nodes (DLN) of anti-CD47–treated MC38-OTIp–bearing mice and cocultured them with OVA-specific OTI T cells. DCs and macrophages were isolated by FACS, and their purity was validated by quantitative RT-PCR using the lineage-defining transcription factor genes *Mafb* (macrophages) and *Zbtb46* (DCs) (**Supplementary Fig. 3a**). We hypothesized that anti-CD47 would increase phagocytosis inside the tumor, leading to migration of antigen-loaded APCs to the DLN, where they would fully mature and cross-prime naive T cells. However, we did not observe significant cross-priming by either macrophages or DCs from the DLN from anti-CD47–treated mice (**Fig. 3b**). In contrast, primary DCs, but not macrophages, harvested from the tumor microenvironment clearly elicited increased activation of T cells after anti-CD47 treatment (**Fig. 3c**). We observed similar effects using macrophages and DCs from mice bearing A20-HA (hemagglutinin expressing) lymphomas after coculture with HA-reactive T cells from CL4 T cell receptor (TCR)-transgenic (Tg) mice, in which the TCR is specific for the HA antigen. We observed augmented T cell cross-priming induced by DCs compared to macrophages, suggesting that anti-CD47 therapy enhances the ability of DCs (but not macrophages) to cross-prime T cells across tumor subtypes (**Supplementary Fig. 4a**). This was also the case when we analyzed parental A20 or MC38 tumors, indicating that DC-mediated cross-priming of T cells specific for naturally expressed tumor antigens was also enhanced following anti-CD47 therapy (**Fig. 3d**,**e**). To assess whether anti-CD47 had a similar impact in an orthotopic tumor model, we implanted TUBO, an oncogenic receptor neu$^+$ mammary tumor, into mammary fat pads of *neu*-transgenic mice,

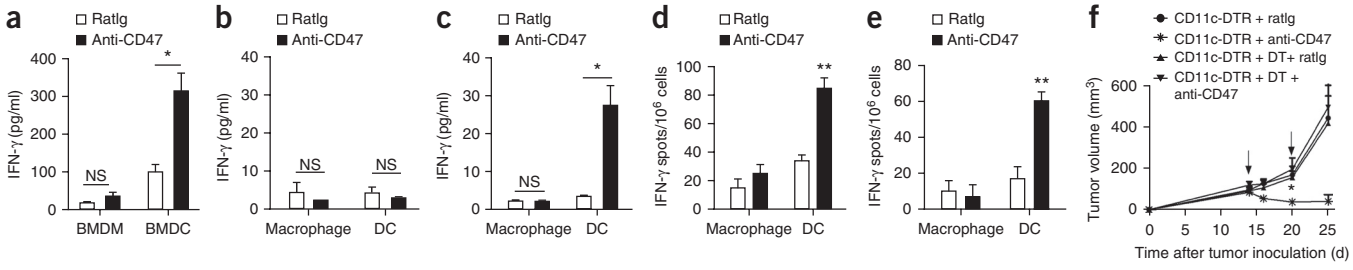

Figure 3 Anti-CD47 triggers the cross-priming ability of DCs. (**a**) BMDCs or bone marrow macrophages were cultured with MC38-OTIp in the presence of fresh granulocyte-macrophage colony–stimulating factor (GM-CSF) and anti-CD47 overnight. Subsequently, purified CD11c$^+$ cells or F4/80$^+$ cells were cocultured with isolated CD8$^+$ T cells from naive OTI mice for 3 d and analyzed by IFN-γ cytometric bead array (CBA). (**b**,**c**) MC38-OTIp–bearing mice ($n = 5$ per group) were treated twice with 50 μg of either anti-CD47 or ratIg on days 11 and 14 intratumorally. Five days after the initial treatment, DLN DCs (**b**) and tumor-infiltrating (**c**) DCs and macrophages were isolated and cocultured with isolated CD8$^+$ T cells from naive OTI mice for 3 d. IFN-γ production was detected by CBA. (**d**,**e**) A20 (**d**) or MC38 (**e**) tumor-bearing C57BL/6 mice ($n = 5$ per group) were treated with 50 μg of either anti-CD47 or ratIg isotype control on day 10. Four days after the antibody treatment, 3×10^4 tumor-infiltrating DCs and macrophages were isolated and cocultured with isolated 3×10^5 CD8$^+$ T cells from A20 (**d**) or MC38 (**e**) tumor-bearing mice. Forty-eight hours later, IFN-γ–producing cells were enumerated by ELISPOT assay. (**f**) Five weeks after the indicated CD11c-DTR bone marrow chimera reconstitution, C57BL/6 mice ($n = 5$ per group) were injected s.c. with 1×10^6 MC38 cells and treated with 50 μg of anti-CD47 or ratIg on days 14 and 20 (indicated by black arrow). Diphtheria toxin or PBS was administrated on the same day as treatment. Data are reported as the means ± s.e.m. $^*P < 0.05$, $^{**}P < 0.01$, $^{***}P < 0.001$ (unpaired Student's *t*-test). One representative experiment out of three independent experiments is depicted.

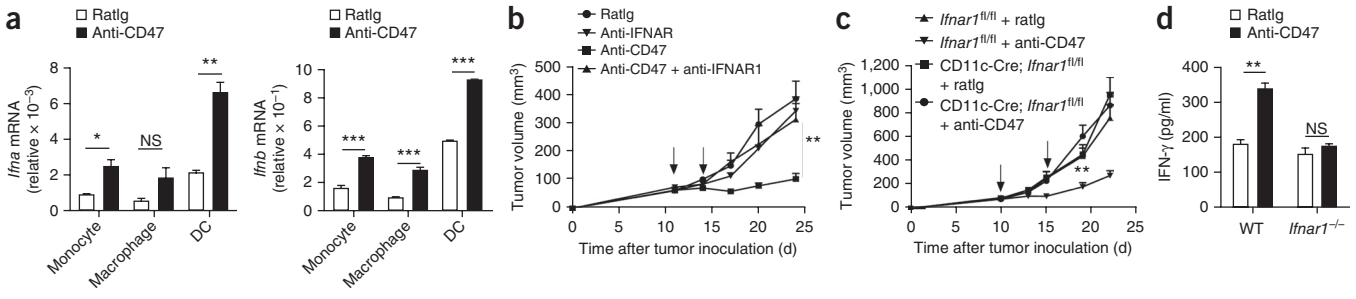

Figure 4 Type I IFNs are induced during anti-CD47 mediated tumor inhibition and required. (**a**) Four days after anti-CD47 or ratIg treatment ($n = 5$ per group), the single-cell suspensions from tumors were sorted into CD45$^+$CD11c$^-$CD11b$^+$Ly6c^{hi} (monocytes), CD45$^+$CD11c$^{-/+}$ CD11b$^+$Ly6c$^-$F4/80$^+$ (macrophages) and CD45$^+$CD11c$^+$CD11b$^{-/+}$Ly6C$^-$F4/80$^-$ (DC) populations. mRNA levels of *Ifna* and *Ifnb* in different cell subsets were quantified by real-time PCR assay. Representative data are reported as mean copy numbers ± s.e.m. after intrasample normalization to the levels of reference gene *Hprt* in three independent experiments. $^*P < 0.05$, $^{**}P < 0.01$, $^{***}P < 0.001$ (unpaired Student's *t*-test). (**b**) C57BL/6 mice ($n = 6$) were injected s.c. with 1×10^6 MC38 cells and treated intratumorally with 50 μg of anti-CD47 or isotype control ratIg on days 11 and 14 (indicated by black arrow). 50 μg anti-IFNAR1 antibody was administered intratumorally on days 0 and 2 after anti-CD47 treatment. (**c**) *Ifnar1*$^{fl/fl}$ and CD11c-Cre; *Ifnar1*$^{fl/fl}$ mice ($n = 6$) were injected s.c. with 1×10^6 MC38 cells and treated with 50 μg of anti-CD47 or ratIg on days 10 and 15 (indicated by black arrow). (**d**) BMDCs from WT mice or *Ifnar1*$^{-/-}$ mice were cultured with MC38-OTIp in the presence of anti-CD47 or ratIg for 16 h. Subsequently, purified CD11c$^+$ cells were cocultured with isolated CD8$^+$ T cells from naive OTI mice for 3 d. IFN-γ production in supernatant was determined by CBA. Data are reported as means ± s.e.m. Tumor growth is reported as the mean tumor size ± s.e.m. over time. $^{**}P < 0.01$; one representative experiment out of three independent experiments is depicted.

which we subsequently treated with anti-CD47 or isotype control mAb. Here again, increased T cell cross-priming by DCs was observed when they were cocultured with CD8$^+$ T cells isolated from TUBO tumor-bearing mice (**Supplementary Fig. 4b**). Together, these findings indicate that anti-CD47 therapy enhances cross-priming of antigen-specific T cells by tumor-resident DCs.

To determine whether anti-CD47–induced DC activation was also required for tumor control, we inoculated tumor-bearing CD11c-diphtheria toxin receptor (*Itgax*-DTR) bone marrow–chimeric (BMC) mice with MC38 cells s.c. and treated them with diphtheria toxin (DT) to deplete DCs during anti-CD47 treatment. The therapeutic effect of CD47 blockade was severely impaired following DC depletion in tumor-bearing mice (**Fig. 3f**). However, selective removal of tumor-associated macrophages by a colony-stimulating factor (CSF1)-blocking mAb had no impact on the antitumor response following CD47 blockade (**Supplementary Fig. 3b**). These data strongly suggest that increased DC cross-priming of cytotoxic T lymphocytes is crucial for the therapeutic effect of anti-CD47 treatment.

Requirement for DC responsiveness to type I IFNs for tumor control

Type I IFNs are known to increase the cross-priming capability of DCs after various antitumor therapies[25–29]. Therefore, we investigated whether type I IFNs were involved in cross-priming induced by CD47 blockade. First, mice with established MC38 tumors were treated with anti-CD47 or isotype control rat Ig. Subsequently, DCs and macrophages were sorted from tumor tissues, and levels of type I IFN mRNA (*Ifna* and *Ifnb)* were determined by quantitative PCR. DCs from mice treated with anti-CD47 expressed more *Ifna* mRNA than DCs from mice treated with rat immunoglobulin (Ig) isotype control. In contrast, anti-CD47 boosted *Ifna* mRNA abundance in

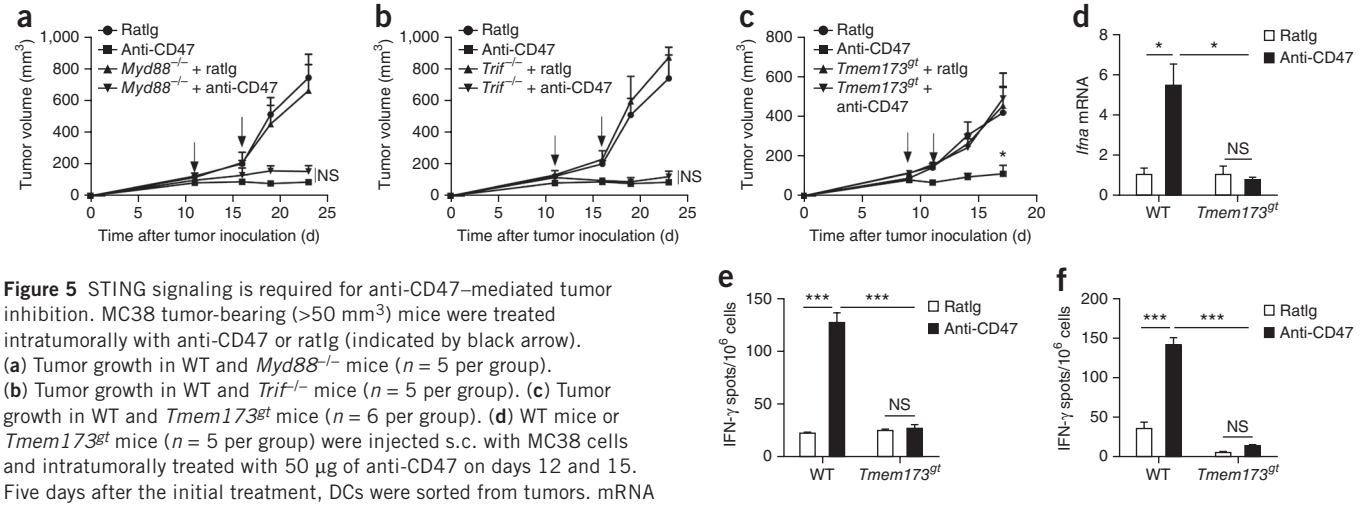

Figure 5 STING signaling is required for anti-CD47–mediated tumor inhibition. MC38 tumor-bearing (>50 mm^3) mice were treated intratumorally with anti-CD47 or ratIg (indicated by black arrow). (**a**) Tumor growth in WT and *Myd88*$^{-/-}$ mice ($n = 5$ per group). (**b**) Tumor growth in WT and *Trif*$^{-/-}$ mice ($n = 5$ per group). (**c**) Tumor growth in WT and *Tmem173*^{gt} mice ($n = 6$ per group). (**d**) WT mice or *Tmem173*^{gt} mice ($n = 5$ per group) were injected s.c. with MC38 cells and intratumorally treated with 50 μg of anti-CD47 on days 12 and 15. Five days after the initial treatment, DCs were sorted from tumors. mRNA levels of *Ifna* were quantified by real-time PCR assay. Representative data are reported as mean copy numbers ± s.e.m. after intrasample normalization to the levels of *Hprt* in three independent experiments. $^*P < 0.05$ (unpaired Student's *t*-test). (**e**) BMDCs from WT mice or *Tmem173*^{gt} mice were cultured with MC38-OTIp in the presence of anti-CD47 or ratIg for 16 h. Subsequently, purified CD11c$^+$ cells were cocultured with purified OTI cells for 2 d. IFN-γ production was determined by ELISPOT assay. (**f**) MC38 tumor–bearing C57BL/6 mice ($n = 5$ per group) were sacrificed 7 d after the final treatment. 2.5×10^5 CD8$^+$ T cells, isolated from DLNs, were stimulated with MC38 tumor cells. The ratio of CD8$^+$ T cells to MC38 was 50:1. IFN-γ–producing cells were enumerated by ELISPOT assay. Result was expressed as number of spots per 1×10^6 CD8$^+$ T cells. Data are reported as means ± s.e.m. $^*P < 0.05$, $^{**}P < 0.01$, $^{***}P < 0.001$ (unpaired Student's *t*-test). One of three experiments is shown.

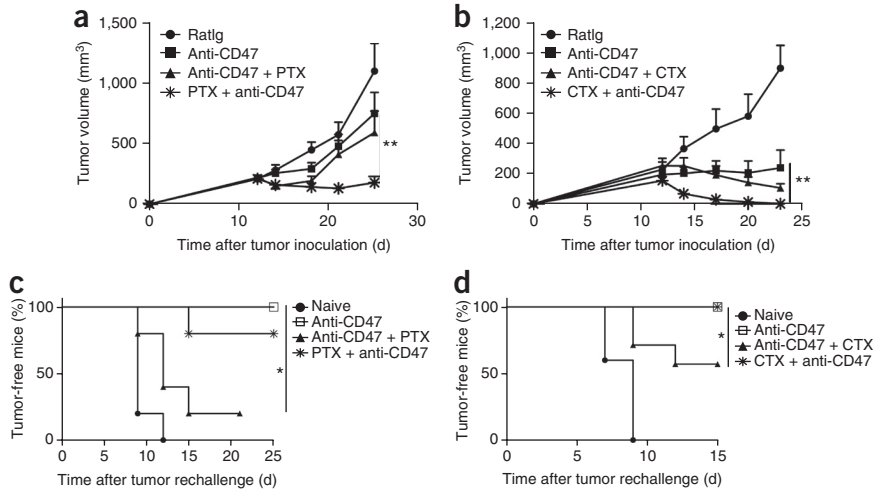

Figure 6 Anti-CD47-mediated immune protection is impaired by some post treatment chemotherapeutics. BALB/c mice ($n = 6$ per group) were injected s.c. with 3×10^6 A20 cells and treated with 50 µg of anti-CD47 on days 12 and 17. Select chemotherapeutic agents were injected i.p. at different time points. (**a**) 40 mg/kg of PTX was injected i.p. in a single dose on day 11 (1 d before anti-CD47) or three doses on days 15, 18 and 21 (starting 3 d after anti-CD47) ($n = 7$ pooled from two experiments). Tumor growth is reported as the mean tumor size ± s.e.m. over time. $^{**}P < 0.01$ (unpaired Student's *t*-test). (**b**) 60 mg/kg of CTX ($n = 5$ per group) was injected i.p. in a single dose on day 11 (1 d before anti-CD47) or three doses on days 15, 18 and 21 (starting 3 d after anti-CD47). Tumor growth is reported as the mean tumor size ± s.e.m. over time. $^{**}P < 0.01$ (two-way analysis of variance). One representative experiment out of two independent experiments is depicted. (**c**,**d**) Treated mice ($n = 7$ per group) had tumors removed by surgery and were rechallenged with 1.5×10^7 A20 cells 1 week after surgery. Percentage of tumor-free mice is shown. $^{*}P < 0.05$ (Mantel-Cox). One representative experiment out of two independent experiments is depicted.

the monocyte and macrophage population by only twofold (**Fig. 4a**). Similar patterns were observed for *Ifnb* mRNA (**Fig. 4a**).

To test whether type I IFNs were required for the anti-CD47 mediated antitumor effect *in vivo*, mice bearing MC38 or A20 tumors were treated with intratumoral injections of IFNAR-blocking antibody on days 0 and 2 after injection with anti-CD47 or isotype control. Blocking type I IFN signaling impaired the therapeutic effect of anti-CD47 (**Fig. 4b** and **Supplementary Fig. 5**), suggesting that type I IFNs are essential for anti-CD47–mediated tumor regression. Given the important role of type I IFNs on DC activation and the importance of DCs in anti-CD47–mediated therapeutic effects, we assessed whether type I IFN signaling specifically in DCs was required for tumor responses following CD47 blockade. To this end, we established MC38 tumors in CD11cCre$^+$; *Ifnar1*$^{fl/fl}$ mice and *Ifnar1*$^{fl/fl}$ mice. Conditional deletion of *Ifnar1* in CD11c$^+$ cells markedly reduced the effect of CD47 blockade on tumor growth (**Fig. 4c**), demonstrating that type I IFN signaling in DCs is necessary for the therapeutic efficacy of anti-CD47. Because CD11c is known to be expressed on cells other than DCs, we performed a DC cross-priming assay using BMDCs. The cross-priming capacity of BMDCs from *Ifnar1*-deficient mice in the presence of anti-CD47 was compromised compared to that of BMDCs from wild-type mice (**Fig. 4d**). Together, these data indicate that type I IFN signaling in DCs plays an integral role in boosting the adaptive immune response to anti-CD47 antibody therapy.

Essential role for cytosolic DNA sensing for cross-priming

Anti-CD47–induced phagocytosis might preferentially target stressed tumor cells expressing high levels of prophagocytic molecules. Substances released by tumor cells engulfed into phagosomes might also promote activation of host APCs[30–32]. For example, tumor-derived danger-associated molecular patterns (DAMPs) engulfed during phagocytosis could initiate type I IFN production by engaging Toll-like receptor–myeloid differentiation factor-88 (TLR-MyD88) sensing pathways in host APCs[31,33]. To determine whether host TLR pathways were required for the antitumor effect of anti-CD47 therapy, we established MC38 tumors in *Myd88*$^{-/-}$ and *Trif*$^{-/-}$ (*Trif* is officially known as *Ticam1*) mice. The inhibition of tumor growth after anti-CD47 treatment was comparable in WT, *Myd88*$^{-/-}$ and *Trif*$^{-/-}$ mice (**Fig. 5a**,**b**), indicating that TLR signaling in host cells is dispensable for the antitumor effect of CD47 blockade. These results also suggest that anti-CD47 activates cross-priming through a TLR-independent pathway.

Recent studies have revealed a cytosolic DNA-sensing pathway involving the endoplasmic reticulum–resident protein stimulator of interferon genes (STING)[34–38]. The STING pathway is also essential for host DC sensing of tumor DNA[39,40]. To determine the role of STING in anti-CD47–mediated antitumor responses, we implanted MC38 tumor cells in flanks of WT and *Tmem173*^{gt} (STING-deficient) mice and monitored tumor growth after treatment with anti-CD47 or isotype control rat Ig. Tumor growth was identical in WT mice treated with isotype-control rat Ig and in *Tmem173*^{gt} mice treated with isotype control rat Ig. However, the antitumor effects of anti-CD47 treatment were completely abrogated in *Tmem173*^{gt} mice compared with WT mice (**Fig. 5c**). Thus, cytosolic DNA sensing through STING is absolutely essential for the antitumor effect of anti-CD47 therapy.

To evaluate whether STING was essential for induction of type I IFN after anti-CD47 therapy, we treated WT or *Tmem173*^{gt} mice bearing MC38 tumors with anti-CD47. Five days later, we measured *Ifna* mRNA expression levels in tumor-infiltrating DCs. We observed a significant induction of *Ifna* transcripts in DCs from WT but not *Tmem173*^{gt} mice following CD47 blockade (**Fig. 5d**). To determine whether the anti-CD47–induced DC cross-priming of CD8$^+$ T cells depends on STING, we conducted a cross-priming assay with BMDCs from WT and *Tmem173*^{gt} mice. The cross-priming capacity of WT but not *Tmem173*^{gt} DCs was significantly increased by coculture with tumor cells and anti-CD47 (**Fig. 5e**). We reached a similar conclusion by IFN-γ ELISPOT assay of purified CD8$^+$ T cells from tumor DLNs of WT and *Tmem173*^{gt} mice treated with anti-CD47; anti-CD47 induced tumor-specific CD8$^+$ T cell IFN-γ production in WT but not *Tmem173*^{gt} mice (**Fig. 5f**). Overall, these results suggest that the STING-dependent cytosolic DNA sensing pathway is essential for anti-CD47–induced antitumor adaptive immune responses.

Chemotherapy influences anti-CD47 effects

Clinical trials of anti-CD47 treatment are underway, but many patients might also have received or continue to receive chemotherapy. As our data reveal an essential role of T cells, and as chemotherapy can suppress

the immune system and kill recently activated immune cells[41,42], chemotherapy may blunt the therapeutic effects of anti-CD47 antibody therapy. Alternatively, chemotherapy may synergize with anti-CD47 by increasing release of antigens and DNA from dying tumor cells. To test whether chemotherapy drugs used for lymphoma synergize with or inhibit anti-CD47 therapy, we combined anti-CD47 treatment with clinically equivalent doses of cyclophosphamide (CTX) or paclitaxel (PTX) to treat large, established A20 tumors in BALB/c mice. PTX (40 mg/kg) or CTX (60 mg/kg) was administered 3 days before or after anti-CD47 treatment. Chemotherapy administered after anti-CD47 treatment did not result in faster tumor regression than anti-CD47 alone (**Fig. 6a**,**b**). To test the impact of chemotherapy on anti-CD47–mediated acute and memory immune responses, all tumors were surgically removed. One week after surgery, mice were rechallenged with 1.5×10^7 A20 cells. All mice whose primary tumor underwent anti-CD47 treatment alone rejected the tumor rechallenge (**Fig. 6c**). In contrast, a majority of the mice treated with anti-CD47 followed by chemotherapy were susceptible to tumor outgrowth after rechallenge (50% of CTX combination mice; 80% of PTX combination mice) (**Fig. 6c**,**d** and **Supplementary Table 1**). This suggests that chemotherapy administered after anti-CD47 therapy had detrimental effects on development of beneficial antitumor memory immune responses.

We speculated that there might be a limited window of time when chemotherapy drugs can effectively reduce tumor burden and induce prophagocytic signals without destroying anti-CD47–induced immunity. To test whether chemotherapy given before anti-CD47 also inhibited immune memory, we injected an identical dose of PTX or CTX 1 day before antibody treatment rather than 3 days after. This single treatment of chemotherapy before anti-CD47 not only synergized with anti-CD47 for tumor control but also preserved the host memory response against relapsing tumors generated by anti-CD47 (100% of CTX combination mice and 80% of PTX combination mice resistant to tumor rechallenge) (**Fig. 6a–c** and **Supplementary Table 1**). Taken together, our results indicate that simple alterations to standard drug administration could have a major impact on primary and memory immune responses to tumors and alter clinical outcomes in response to immunomodulatory anti-CD47 antibody therapy.

DISCUSSION

Previous publications suggested that anti-CD47 therapy exerts antitumor activity by blocking antiphagocytic signaling, leading to tumor cell death by macrophage-mediated phagocytosis in a manner independent of adaptive immunity[12,16,18]. In contrast, here we reveal that in immune-competent mice, the therapeutic effect of low doses of anti-CD47 largely depends on DC cross-priming of $CD8^+$ T cells. Within DCs, STING-mediated sensing of DNA, which drives type I IFN production, is also required. Finally, timely combination of conventional therapeutics with immunotherapy can boost the host response to control or even eradicate tumors and prevent future relapse.

Potential reasons for the differences between our conclusions and those of previous studies include differences in the preclinical animal models used[12,16]. Most previous studies used tumor xenograft models, which are widely used as preclinical models and are an integral part of the US Food and Drug Administration approval process. Anti–human CD47 showed impressive efficacy toward xenografted human tumor cells (especially lymphoma and leukemia) in NSG mice (nonobese diabetic (NOD) severe combined immunodeficiency (SCID) interleukin-2 receptor γ chain–deficient mice without T and B cells)[16,18]. By comparing syngeneic mouse tumors in WT and T cell–deficient nude mice, we revealed a role for T cells in the therapeutic effects of anti-CD47. Several factors could explain the apparently strong role for phagocytosis observed in xenograft models. First, upon implantation in an NSG model human CD47 binds to NSG mouse SIRPα due to a germline SIRPα mutation of these mice, whereas human CD47 could not bind well to SIRPα in other strains of mice, including BALB/c and C57BL/6 (refs. 43,44). This unique binding between human CD47 and NOD mouse SIRPα on activated innate cells makes them more susceptible to antibody blockade. Second, in xenograft models, the therapeutic effect of anti–human CD47 was often achieved at much higher doses (for example, 200 μg daily for consecutive 14 d) than the current study[12]. We did observe better tumor control when a higher dose of anti–mouse CD47 antibody was used in the nude mouse model. Lastly, in a syngeneic setting, anti-CD47 will bind both healthy and malignant cells that express CD47. However, in the xenograft model, only tumor cells express human CD47.

Our work may differ from published works in another way: using an *in vitro* serum-free assay, a recent study showed that phagocytosis of human tumor cells after anti-human CD47 treatment is mainly attributed to mouse BMDMs, whereas the contribution of BMDCs is almost undetectable[24]. Consistently across multiple experiments, enhancement of cross-priming by macrophages was observed in response to anti-CD47. Conversely, we observed that both BMDCs and primary DCs are more potent than BMDMs and primary macrophages for cross-priming T cells. To explain this contradiction, we have observed that culturing BMDCs without serum results in increased apoptosis and malfunction of the DCs, which could ultimately impair their cross-priming capacity (**Supplementary Fig. 6**). Supplemented with serum, BMDCs recovered their ability to cross-prime *in vitro*. Furthermore, *ex vivo*–isolated DCs are more able to cross-prime CTL than are *ex vivo* isolated macrophages after anti-CD47 treatment. Finally, deletion of DCs *in vivo* limits the antitumor effects of anti-CD47 and the antitumor effect of the anti-CD47 depends on IFNAR on $CD11c^+$ cells. Thus, our data clearly demonstrate in an immune-competent syngeneic host that the therapeutic effect of CD47 blockade requires functional DCs.

Another point related to the clinical scenario is tumor immunogenicity. Accumulating evidence suggests that the response to immunotherapies is often reliant on the immunogenicity of a tumor, with tumors bearing high loads of somatic mutations showing greater responsiveness than tumors bearing relatively few somatic mutations. Highly mutated tumors probably express higher numbers of neoantigens that can be better recognized and rejected by host T cells, for example, when the CTLA-4 or PD-1 co-inhibitory pathways are blocked by therapeutic antibodies[45,46]. As such, it is possible that anti-CD47 treatment could possibly have more impact on immunogenic tumors than on nonimmunogenic tumors.

Finally, standard chemotherapy can have major impacts on anti-CD47 therapy efficacy. Prior studies have shown that chemotherapy can lead to increased expression of cell surface calreticulin on tumor cells[42]. Thus, chemotherapy-mediated upregulation of cell surface calreticulin, a prophagocytic signal, may potentially augment the efficacy of anti-CD47 antibodies by propagating STING signaling. In addition, chemotherapy may lead to increased infiltration of APCs, including DCs and macrophages, to tumor sites[47,48]. However, properly inducing $CD8^+$ T cell–mediated tumor regression requires careful design of sequence and doses for both chemotherapy drugs and anti-CD47, as inappropriate combination treatments of antibody plus chemotherapy may have negative effects on the host immune

response to tumor antigens. Thus future clinical trials involving anti-CD47 treatment and standard-of-care chemotherapy must be properly timed and tested, as both synergy and antagonism will be time and dose dependent. In conclusion, understanding the mechanisms by which CD47 blockade interfaces with host antitumor immunity will yield important information for designing new treatments using combinations of anti-CD47 with chemotherapeutics and other immunomodulatory antibodies.

METHODS

Methods and any associated references are available in the online version of the paper.

Note: Any Supplementary Information and Source Data files are available in the online version of the paper.

ACKNOWLEDGMENTS

We thank R. Schreiber (Washington University, St. Louis) for providing us with anti-IFNAR antibody. *Ifnar1*$^{fl/fl}$ mice were kindly provided by U. Kalinke from the Institute for Experimental Infection Research. Anti-IFN-γ neutralizing mAb (clone R46A2) was provided by Z. Qin (the Institute of Biophysics, CAS). Some anti-CD47 antibody (clone MIAP301) was provided by W. Frazier (Washington University, St. Louis). This research was in part supported by US National Institutes of Health grants CA141975 and C134563 to Y.-X.F., the National 12.5 major project of China (No. 2012ZX10001006002004) to Y.-X.F. and H.P., Chinese Academy of Sciences grant XDA09030303 and 2012CB910203 to Y.-X.F. and a Dean's Award from Washington University to W.A.F.

AUTHOR CONTRIBUTIONS

X.L., Y.P., H.X. and M.M.X. performed experiments. L.D., J.K., W.A.F. and H.P. provided reagents. X.L., M.M.X. and Y.-X.F. designed and organized experiments. K.C., J.K. and H.P. edited the manuscript. X.L., M.M.X. and Y.-X.F. wrote the paper. Y.-X.F. guided the work.

COMPETING FINANCIAL INTERESTS

The authors declare competing financial interests: details accompany the online version of the paper.

1. Gardai, S.J. *et al.* Cell-surface calreticulin initiates clearance of viable or apoptotic cells through trans-activation of LRP on the phagocyte. *Cell* **123**, 321–334 (2005).
2. Chao, M.P. *et al.* Calreticulin is the dominant pro-phagocytic signal on multiple human cancers and is counterbalanced by CD47. *Sci. Transl. Med.* **2**, 63ra94 (2010).
3. Chao, M.P., Majeti, R. & Weissman, I.L. Programmed cell removal: a new obstacle in the road to developing cancer. *Nat. Rev. Cancer* **12**, 58–67 (2012).
4. Oldenborg, P.A. *et al.* Role of CD47 as a marker of self on red blood cells. *Science* **288**, 2051–2054 (2000).
5. Blazar, B.R. *et al.* CD47 (integrin-associated protein) engagement of dendritic cell and macrophage counterreceptors is required to prevent the clearance of donor lymphohematopoietic cells. *J. Exp. Med.* **194**, 541–549 (2001).
6. Barclay, A.N. & Van den Berg, T.K. The interaction between signal regulatory protein alpha (SIRPα) and CD47: structure, function, and therapeutic target. *Annu. Rev. Immunol.* **32**, 25–50 (2014).
7. Yamao, T. *et al.* Negative regulation of platelet clearance and of the macrophage phagocytic response by the transmembrane glycoprotein SHPS-1. *J. Biol. Chem.* **277**, 39833–39839 (2002).
8. Olsson, M., Bruhns, P., Frazier, W.A., Ravetch, J.V. & Oldenborg, P.A. Platelet homeostasis is regulated by platelet expression of CD47 under normal conditions and in passive immune thrombocytopenia. *Blood* **105**, 3577–3582 (2005).
9. Tsai, R.K. & Discher, D.E. Inhibition of "self" engulfment through deactivation of myosin-II at the phagocytic synapse between human cells. *J. Cell Biol.* **180**, 989–1003 (2008).
10. Poels, L.G. *et al.* Monoclonal antibody against human ovarian tumor-associated antigens. *J. Natl. Cancer Inst.* **76**, 781–791 (1986).
11. Jaiswal, S. *et al.* CD47 is upregulated on circulating hematopoietic stem cells and leukemia cells to avoid phagocytosis. *Cell* **138**, 271–285 (2009).
12. Majeti, R. *et al.* CD47 is an adverse prognostic factor and therapeutic antibody target on human acute myeloid leukemia stem cells. *Cell* **138**, 286–299 (2009).
13. Rendtlew Danielsen, J.M., Knudsen, L.M., Dahl, I.M., Lodahl, M. & Rasmussen, T. Dysregulation of CD47 and the ligands thrombospondin 1 and 2 in multiple myeloma. *Br. J. Haematol.* **138**, 756–760 (2007).
14. Chan, K.S. *et al.* Identification, molecular characterization, clinical prognosis, and therapeutic targeting of human bladder tumor-initiating cells. *Proc. Natl. Acad. Sci. USA* **106**, 14016–14021 (2009).
15. Chan, K.S., Volkmer, J.P. & Weissman, I. Cancer stem cells in bladder cancer: a revisited and evolving concept. *Curr. Opin. Urol.* **20**, 393–397 (2010).
16. Chao, M.P. *et al.* Anti-CD47 antibody synergizes with rituximab to promote phagocytosis and eradicate non-Hodgkin lymphoma. *Cell* **142**, 699–713 (2010).
17. Willingham, S.B. *et al.* The CD47-signal regulatory protein α (SIRPa) interaction is a therapeutic target for human solid tumors. *Proc. Natl. Acad. Sci. USA* **109**, 6662–6667 (2012).
18. Chao, M.P. *et al.* Therapeutic antibody targeting of CD47 eliminates human acute lymphoblastic leukemia. *Cancer Res.* **71**, 1374–1384 (2011).
19. Chao, M.P. *et al.* Extranodal dissemination of non-Hodgkin lymphoma requires CD47 and is inhibited by anti-CD47 antibody therapy. *Blood* **118**, 4890–4901 (2011).
20. Soto-Pantoja, D.R. *et al.* CD47 in the tumor microenvironment limits cooperation between antitumor T-cell immunity and radiotherapy. *Cancer Res.* **74**, 6771–6783 (2014).
21. Lee, Y. *et al.* Therapeutic effects of ablative radiation on local tumor require CD8+ T cells: changing strategies for cancer treatment. *Blood* **114**, 589–595 (2009).
22. Brown, E.J. & Frazier, W.A. Integrin-associated protein (CD47) and its ligands. *Trends Cell Biol.* **11**, 130–135 (2001).
23. Weiskopf, K. *et al.* Engineered SIRPα variants as immunotherapeutic adjuvants to anticancer antibodies. *Science* **341**, 88–91 (2013).
24. Tseng, D. *et al.* Anti-CD47 antibody-mediated phagocytosis of cancer by macrophages primes an effective antitumor T-cell response. *Proc. Natl. Acad. Sci. USA* **110**, 11103–11108 (2013).
25. Burnette, B.C. *et al.* The efficacy of radiotherapy relies upon induction of type I interferon-dependent innate and adaptive immunity. *Cancer Res.* **71**, 2488–2496 (2011).
26. Diamond, M.S. *et al.* Type I interferon is selectively required by dendritic cells for immune rejection of tumors. *J. Exp. Med.* **208**, 1989–2003 (2011).
27. Fuertes, M.B. *et al.* Host type I IFN signals are required for antitumor CD8$^+$ T cell responses through CD8α$^+$ dendritic cells. *J. Exp. Med.* **208**, 2005–2016 (2011).
28. Stagg, J. *et al.* Anti-ErbB-2 mAb therapy requires type I and II interferons and synergizes with anti-PD-1 or anti-CD137 mAb therapy. *Proc. Natl. Acad. Sci. USA* **108**, 7142–7147 (2011).
29. Yang, X. *et al.* Targeting the tumor microenvironment with interferon-β bridges innate and adaptive immune responses. *Cancer Cell* **25**, 37–48 (2014).
30. Chen, G.Y. & Nunez, G. Sterile inflammation: sensing and reacting to damage. *Nat. Rev. Immunol.* **10**, 826–837 (2010).
31. Desmet, C.J. & Ishii, K.J. Nucleic acid sensing at the interface between innate and adaptive immunity in vaccination. *Nat. Rev. Immunol.* **12**, 479–491 (2012).
32. Kono, H. & Rock, K.L. How dying cells alert the immune system to danger. *Nat. Rev. Immunol.* **8**, 279–289 (2008).
33. O'Neill, L.A., Golenbock, D. & Bowie, A.G. The history of Toll-like receptors—redefining innate immunity. *Nat. Rev. Immunol.* **13**, 453–460 (2013).
34. Ishikawa, H. & Barber, G.N. STING is an endoplasmic reticulum adaptor that facilitates innate immune signalling. *Nature* **455**, 674–678 (2008).
35. Ishikawa, H., Ma, Z. & Barber, G.N. STING regulates intracellular DNA-mediated, type I interferon-dependent innate immunity. *Nature* **461**, 788–792 (2009).
36. Li, X.D. *et al.* Pivotal roles of cGAS-cGAMP signaling in antiviral defense and immune adjuvant effects. *Science* **341**, 1390–1394 (2013).
37. Sun, L., Wu, J., Du, F., Chen, X. & Chen, Z.J. Cyclic GMP-AMP synthase is a cytosolic DNA sensor that activates the type I interferon pathway. *Science* **339**, 786–791 (2013).
38. Wu, J. *et al.* Cyclic GMP-AMP is an endogenous second messenger in innate immune signaling by cytosolic DNA. *Science* **339**, 826–830 (2013).
39. Woo, S.R. *et al.* STING-dependent cytosolic DNA sensing mediates innate immune recognition of immunogenic tumors. *Immunity* **41**, 830–842 (2014).
40. Deng, L. *et al.* STING-dependent cytosolic DNA sensing promotes radiation-induced type I interferon-dependent antitumor immunity in immunogenic tumors. *Immunity* **41**, 843–852 (2014).
41. Obeid, M. *et al.* Ecto-calreticulin in immunogenic chemotherapy. *Immunol. Rev.* **220**, 22–34 (2007).
42. Obeid, M. *et al.* Calreticulin exposure dictates the immunogenicity of cancer cell death. *Nat. Med.* **13**, 54–61 (2007).
43. Takenaka, K. *et al.* Polymorphism in *Sirpa* modulates engraftment of human hematopoietic stem cells. *Nat. Immunol.* **8**, 1313–1323 (2007).
44. Yamauchi, T. *et al.* Polymorphic *Sirpa* is the genetic determinant for NOD-based mouse lines to achieve efficient human cell engraftment. *Blood* **121**, 1316–1325 (2013).
45. Matsushita, H. *et al.* Cancer exome analysis reveals a T-cell-dependent mechanism of cancer immunoediting. *Nature* **482**, 400–404 (2012).
46. Snyder, A. *et al.* Genetic basis for clinical response to CTLA-4 blockade in melanoma. *N. Engl. J. Med.* **371**, 2189–2199 (2014).
47. Ma, Y. *et al.* Anticancer chemotherapy-induced intratumoral recruitment and differentiation of antigen-presenting cells. *Immunity* **38**, 729–741 (2013).
48. Ma, Y. *et al.* CCL2/CCR2-dependent recruitment of functional antigen-presenting cells into tumors upon chemotherapy. *Cancer Res.* **74**, 436–445 (2014).

ONLINE METHODS

Mice. Six- to eight-week-old female C57BL/6J mice were purchased from Harlan or Jackson Laboratory. Six- to eight-week-old female BALB/c mice were purchased from Charles River Laboratories in China. *Myd88*$^{-/-}$, *Trif*$^{-/-}$, *Tmem173*^{gt}, OT-I CD8^{+} T cell receptor (TCR)-Tg, CD11c-Cre-Tg, CD11c(*Itgax*)-DTR and BALB/c-Tg (*MMTV-neu*) mice were purchased from The Jackson Laboratory. *Ifnar1*$^{fl/fl}$ mice were kindly provided by U. Kalinke from the Institute for Experimental Infection Research, Hanover, Germany. All the mice were maintained under specific pathogen–free conditions and used between 6–12 weeks of age in accordance to the animal experimental guidelines set by the Institutional Animal Care and Use Committee of the University of Chicago and Institute of Biophysics, CAS.

Cell lines and reagents. All cell lines were characterized by short tandem repeat analysis (STR) profiling and tested free of mycoplasma contamination. MC38 is a murine colon adenocarcinoma cell line. A20 is a murine B cell lymphoma cell line. MC38-OTIp was sorted and subcloned after MC38 cells were stably transduced with retrovirus expressing mouse EGFRVIII-OTIp (peptide epitope for OTI). A20-HA was selected as a single clone after being transduced by retrovirus expressing hemagglutination antigen (HA). TUBO was cloned from a spontaneous mammary tumor in a BALB *neu* Tg mouse[49]. Anti-IFN-γ neutralizing mAb (clone R46A2) was provided by Dr. Zhihai Qin (the Institute of Biophysics, CAS). Anti-CSF1 neutralizing mAb (5A1) and anti-mIFNAR1 neutralizing mAb (clone MAR1-5A3) were purchased from BioXcell (West Lebanon, NH). Anti-CD47 antibody (clone MIAP301) was initially purchased from eBioscience or BioLegend and then provided by Dr. William Frazier (Washington University, St. Louis). It is a rat-derived antibody that specifically recognizes mouse CD47 and blocks mouse SIRPα binding[50]. SIRPα-hIg, anti-CD8 depleting antibody (clone TIB210) and anti-CD4 depleting antibody (clone GK1.5) were produced in house. The endotoxin level for Ab and fusion protein is lower than 0.2 EU (Endotoxin Units)/μg of protein. Chemotherapeutic agents cyclophosphamide (CTX), paclitaxel (PTX) and doxorubicin (DOX) were purchased from Sigma and prepared according to the manufacturers' recommendations.

Tumor growth and treatments. 2–5 × 10^{6} A20 or 1 × 10^{6} MC38 tumor cells were s.c. injected into the flank of mice. Tumor volumes were measured by length (a) and width (b) and calculated as tumor volume = $ab^2/2$. Tumors, allowed to grow for 7–14 d to reach 50 mm^{3}, were treated by anti-CD47 or rat Ig intratumorally or i.p. For Sirpα-hIg treatment, 5 × 10^{6} A20 tumor cells were s.c. injected into the flank of mice. Tumors were allowed to grow for 14 d and treated by Sirpα-hIg or human Ig intratumorally. For CD8 or CD4 depletion experiments, 200–300 μg of anti-CD8 antibody (clone TIB210) or anti-CD4 (clone GK1.5) was injected i.p. at the same time as anti-CD47 treatment. For the IFN-γ neutralizing experiment, 300 μg of anti-mouse IFN-γ antibody (clone R46A2) was injected i.p. on the day of anti-CD47 treatment. For type I IFN blockade experiments, 50 μg anti-IFNAR1 mAb was intratumorally injected on day 0 and 2 after anti-CD47 Ab. For the CSF1 neutralizing experiment, 100 μg of anti-mouse CSF1 antibody (clone 5A1) was injected i.t. on the same day of anti-CD47 treatment. For chemotherapeutic agent combination, 60 mg/kg of CTX, 40 mg/kg of PTX or 15 mg/kg of DOX were administered i.p. at the indicated times.

Production of Sirpα-hIg fusion protein. Sirpα-hIg was generated as previously[23]. Generally speaking, a plasmid encoding the DNA sequence of Sirpa was synthesized by OriGene technology company. The DNA was then cloned into the pEE12.4 expression plasmid (Lonza, Basel, Switzerland) between the IgG IgGκ leading sequence and the human IgG1 Fc sequence using BsiWI and BstBI. The SIRPa-hIg fusion protein was transiently expressed in FreeStyle 293-F cells.

Generation of bone marrow chimeras. WT mice were lethally irradiated with a single dose of 1,000 rads. The next day, irradiated mice were adoptively transferred with 2–3 × 10^{6} CD11c-DTR Tg donor bone marrow cells. Mice were maintained on sulfamethoxazole and trimethoprim (Bactrim) antibiotics diluted in drinking water for 5 weeks after reconstitution. Mice were injected with tumor cells 5–6 weeks post reconstitution.

***In vitro* culture and function assay of BMDCs and BMDMs.** Single-cell suspensions of bone marrow cells were obtained from C57BL/6J, *Tmem173*^{gt} or *Infar1*$^{-/-}$ mice. The cells were placed in 10-cm Petri dishes and cultured in RPMI-1640 medium containing 10% FBS, supplemented with 20 ng/ml GM-CSF or M-CSF. Fresh media with GM-CSF or M-CSF was added into culture on day 3. BMDCs and BMDMs were harvested for a stimulation assay on day 7. BMDCs or BMDMs were added and cocultured with MC38-OTIp cells at a ratio of 1:1 in the presence of fresh GM-CSF with or without 10 μg/ml anti-CD47 Ab overnight. Subsequently CD11c^{+} cells and F4/80^{+} cells purified by FCS sorting were incubated with isolated CD8^{+} T cells from naive OT-I mice for 3 d.

T cell isolation. OTI naive CD8^{+} T cells were isolated from lymph nodes and spleen of 6-to 12-week-old mice. Selection was carried out with a negative CD8 isolation kit (Stemcell Technologies) following the manufacturer's instructions.

RNA extraction and quantitative real-time RT-PCR. Total RNA from 5 × 10^{4} sorted tumor infiltrating monocytes, macrophages and DCs were extracted with the RNeasy Micro Kit (QIAGEN) and reverse-transcribed with Seniscript Reverse Transcription Kit (QIAGEN). Real-time RT-PCR was performed with SSoFast EvaGreen supermix (Bio-Rad) according to the manufacturer's instructions and with different primer sets on StepOne Plus (Applied Biosystems). Data were normalized by the level of HPRT expression in each individual sample. The $2^{-\Delta\Delta Ct}$ method was used to calculate relative expression changes.

Tumor digestion. Tumor tissues were excised on day 5 after anti-CD47 and digested with 1 mg/ml collagenase IV (Sigma) and 100 mg/ml DNaseI (Sigma) in the incubator with 5% CO_2. After 30 min, tumors were passed through a 70-μm cell strainer to remove large pieces of undigested tumor. Tumor-infiltrating cells were washed twice with PBS containing 2 mM EDTA.

Measurement of IFN-γ–secreting CD8+ T cells by ELISPOT assay. For bone marrow CD11c^{+} cell functional assays, 2 × 10^{4} purified CD11c^{+} or F4/80^{+} cells were incubated with isolated CD8^{+} T cells from naive OTI mice with EasySep Mouse CD8α Positive Selection Kit (Stemcell Technologies) for 3 d at the ratio of 1:10. For tumor-specific CD8^{+} T cell functional assays in the MC38-OTIp model, 5 d after anti-CD47 treatment, tumor DLNs were removed and CD8^{+} T cells were purified. 2 × 10^{5} CD8^{+} T cells were incubated with BMDCs at the ratio of 10:1 for 48 h with or without 5 μg/ml OTI peptide (SIINFEKL). For tumor-specific CD8^{+} T cell functional assays in the MC38 and A20 models, 5 days after anti-CD47 treatment, tumor DLNs were removed. DLN cells were re-stimulated with A20 or MC38. A 96-well HTS-IP plate (Millipore) was precoated with anti–IFN-γ antibody (eBioscience) with a 1:250 dilution overnight at 4 °C. After coculture, cells were removed, 2 μg/ml biotinylated anti–IFN-γ antibody (eBioscience) with a 1:250 dilution was added, and the plate was incubated for 2 h at room temperature or overnight at 4 °C. Avidin-horseradish peroxidase (BD Pharmingen) with a 1:1,000 dilution was then added and the plate was incubated for 1 h at room temperature. The cytokine spots of IFN-γ were developed according to product protocol (Millipore).

***Ex vivo* DC cross-presentation assay.** MC38-OTIp bearing mice were treated with 50 μg of rat Ig or anti-CD47 mAb intratumoral injection on days 11 and 14. Five days later, draining lymph node and tumor were digested and DCs or macrophages were purified by FACS sorting. Approximately 5 × 10^{4} DCs were mixed together with purified 5 × 10^{5} OTI T cells for 3 d. The supernatants were collected, and IFN-γ was measured by Flex Set CBA assay (BD Bioscience).

A20-HA–bearing mice were treated with 50 μg of rat Ig or anti-CD47 intratumoral injection on day 10. Four days later, draining lymph nodes were digested and DCs or macrophages were purified by FACS sorting. Approximately 4 × 10^{3} DCs or macrophages were mixed together with purified 2 × 10^{4} CL4 T cells for 2 d. IFN-γ–producing cells were enumerated by ELISPOT assay.

For tumor-endogenous antigen, A20- or MC38- or TUBO-bearing mice were treated with 50 μg of rat Ig or anti-CD47 intratumorally. Four days later, tumors were digested and DCs or macrophages were purified by FACS sorting. Approximately 3 × 10^{4} DCs were mixed together with purified 3 × 10^{5} CD8^{+} T cells isolated from draining lymph node of mice that had been inoculated with

doi:10.1038/nm.3931

freeze-thawed tumor cells. After 48 h, IFN-γ–producing cells were enumerated by ELISPOT assay.

Flow cytometric sorting and analysis. Single-cell suspensions were blocked with anti-FcR (clone 2.4G2, BioXcell) and then stained with antibodies (1:400 dilution) against CD11c (Clone N418), CD11b (Clone M1/70), Ly6C (Clone HK1.4), Ly6G (Clone1A8), F4/80 (Clone BM8) and CD45 (Clone 30-F11), and 7-AAD. Cells were sorted on a FACSAria II Cell Sorter (BD). For the Mouse IFN-γ Flex Set CBA assay, IFN-γ detection in the supernatants was performed on a FACSCalibur Flow Cytometer (BD). Data were analyzed with FlowJo Software (TriStar).

Primer sequences for real-time PCR. Primer sequences for quantitative real-time PCR were as follows: *infb* forward 5′-TGAACTCCACCAGCAGACA-3′, *infb* reverse 5′-ACCACCATCCAGGCGTAG-3′; *infa1* forward 5′-TCCCCTGACCCAGGAAGATGCC-3′, *infa1* reverse 5′-ATTGGCAGAGGAAGACAGGGCT-3′; *hprt* forward 5′-TGAAGAGCTACTGTAATGATCAGTCA-3′, *hprt* reverse 5′-AGCAAGCTTGCAACCTTAACCA-3′. *mafB* forward 5′- TAGAAGACACAGCAGCAAGACT-3′, *mafB* reverse 5′- GACGCACGCATCACAGAG-3′; *Zbtb46* forward 5′-TCCTTCTGAGTTCTTCTGATTGAG-3′, *Zbtb46* reverse 5′-AGGTTGATGTAGGCTTGATTGT-3′.

Statistical analyses. No statistical method was used to predetermine sample size. Mice were assigned at random to treatment groups for all mouse studies and, where possible, mixed among cages. There were no mice excluded from experiments. The investigators were blinded to group allocation during the experiment and when assessing the tumor size with calipers. Experiments were repeated two to three times. Data were analyzed using Prism 5.0 software (GraphPad) and presented as mean values ± s.e.m. The *P* values were assessed using two-tailed unpaired Student's *t*-test or two-way analysis of variance with *P* values considered significant as follows: $*P < 0.05$; $**P < 0.01$ and $***P < 0.001$. For tumor-free mice frequency, statistics were done with the log-rank (Mantel-Cox) test.

49. Rovero, S. *et al.* DNA vaccination against rat her-2/Neu p185 more effectively inhibits carcinogenesis than transplantable carcinomas in transgenic BALB/c mice. *J. Immunol.* **165**, 5133–5142 (2000).
50. Oldenborg, P.A., Gresham, H.D. & Lindberg, F.P. CD47-signal regulatory protein α (SIRPα) regulates Fcγ and complement receptor-mediated phagocytosis. *J. Exp. Med.* **193**, 855–862 (2001).